Oxidation–Reduction Potentials of the Methane Monooxygenase Hydroxylase Component from *Methylosinus trichosporium* OB3b†

Kim E. Paulsen,‡ Yi Liu,§ Brian G. Fox,‖ John D. Lipscomb,*,§ Eckard Münck,‖ and Marian T. Stankovich*,‡

Departments of Chemistry and Biochemistry, University of Minnesota, Minneapolis, Minnesota 55455, and Department of Chemistry, Carnegie Mellon University, Pittsburgh, Pennsylvania 15213

Received July 30, 1993; Revised Manuscript Received November 3, 1993⊕

ABSTRACT: Methane monooxygenase (MMO) isolated from *Methylosinus trichosporium* OB3b consists of hydroxylase (MMOH), reductase (MMOR), and "B" (MMOB) protein components. MMOH contains two oxygen-bridged dinuclear iron clusters that are the sites of O_2 activation and hydrocarbon oxidation. Each cluster can be stabilized in diferric [Fe(III)·Fe(III)], mixed-valence [Fe(II)·Fe(III)], and diferrous [Fe(II)·Fe(II)] redox states. We have correlated the EPR spin quantitation of the $S = {}^1/_2$ mixed-valence state with the system electrode potential to determine both formal redox potential values for MMOH at 4 °C: $E_1°' = +76 \pm 15$ mV and $E_2°' = +21 \pm 15$ mV ($E_m = +48$ mV, 61% maximum mixed-valence state). Complementary Mössbauer studies of ^{57}Fe-enriched MMOH allowed all three redox states to be quantitated simultaneously in individual samples and revealed that the distribution of redox states was in accord with the measured potential values. EPR spectra of partially reduced MMOH showed that the apparent midpoint potential values of MMOH–MMOR, MMOH–MMOR–MMOB, and MMOH–MMOR–MMOB–substrate complexes were slightly more positive than that of MMOH alone. In contrast, the MMOH–MMOB complex appeared to have a substantially more negative redox potential. The formal redox potential values of the latter complex were determined to be $E_1°' = -52 \pm 15$ mV and $E_2°' = -115 \pm 15$ mV, respectively, at 4 °C ($E_m = -84$ mV, 65% maximum mixed-valence state). This negative 132-mV shift in the midpoint potential of MMOH coupled to MMOB binding suggests that MMOB binds $\approx 10^4$ more strongly to the diferric state of MMOH than to the diferrous state. Since the potential shift is strongly negative, and since a nearly constant separation between the two formal potential values of MMOH is maintained when MMOB binds, the role of the MMOB–MMOH complex must not be to thermodynamically stabilize the formation of the diferrous cluster which is the form that reacts with O_2 during catalysis. However, MMOB binding may provide kinetic stabilization of the diferrous state and/or modulation of the interaction of MMOH with O_2 and hydrocarbon substrates. Such roles may be effected through cyclic association and dissociation of the MMOB–MMOH complex as MMOH oscillates between redox states during catalysis, thereby dynamically altering the affinity of this complex.

The soluble methane monooxygenase (MMO)[1] from the type II methanotrophic bacterium *Methylosinus trichosporium* OB3b catalyzes the NAD(P)H- and O_2-dependent hydroxylation of methane (Higgins et al., 1980; Fox & Lipscomb, 1990):

$$CH_4 + NAD(P)H + O_2 + H^+ \rightarrow CH_3OH + NAD(P)^+ + H_2O$$

The enzyme consists of three protein components: a 245-kDa hydroxylase (MMOH) containing two oxygen-bridged dinuclear iron clusters; a 15.8-kDa component B (MMOB) containing no cofactors or metals; and a 39.7-kDa reductase (MMOR) containing FAD and a [2Fe-2S] cluster (Fox et al., 1989). The diiron cluster of the resting MMOH is in the diferric [Fe(III)·Fe(III)] state, but it can accept one or two electrons to yield the mixed-valence [Fe(II)·Fe(III)] or diferrous [Fe(II)·Fe(II)] state, respectively (Fox et al., 1988). Although all three components are required for efficient multiple turnover coupled to NADH, the fully reduced MMOH in the absence of the other components is capable of a single turnover to yield the same products as the reconstituted system (Fox et al., 1989; Froland et al., 1992). This result shows that the diiron cluster of MMOH is both the site of oxygen activation and the site of hydrocarbon oxidation. This conclusion was confirmed by the demonstration that diferric MMOH could catalyze H_2O_2-dependent turnover of typical MMO substrates in the absence of the other components and O_2 (Andersson et al., 1991).

Despite the catalytic competence of MMOH alone, the other components exert various effects on the rate and course of the reaction, apparently as a consequence of forming stable complexes with MMOH. In particular, MMOB has been shown to form a complex with MMOH which alters the structure of the diiron cluster environment (Fox et al., 1991) and which changes the distribution of products observed from substrates more complex than methane (Froland et al., 1992).

† This work was supported by NIH Grants GM29344 (to M.T.S.), GM40466 (to J.D.L.), and GM22701 (to E.M.).

* Authors to whom correspondence should be addressed. J.D.L.: Department of Biochemistry, University of Minnesota, 4-225 Millard Hall, Minneapolis, MN 55455. Telephone: (612)-625-6454. FAX: (612)-625-2163. M.T.S.: Department of Chemistry, University of Minnesota, Kolthoff and Smith Halls, Minneapolis, MN 55455. Telephone: (612)-624-1019. FAX: (612)-626-7541.

‡ Department of Chemistry, University of Minnesota.

§ Department of Biochemistry, University of Minnesota.

‖ Department of Chemistry, Carnegie Mellon University.

⊕ Abstract published in *Advance ACS Abstracts,* January 1, 1994.

[1] Abbreviations: $E_1°'$, formal potential value for first electron transfer to the diiron cluster; $E_2°'$, formal potential value for second electron transfer to the cluster; E_m, midpoint potential value for overall two electron transfer to the cluster; K_d, dissociation constant; MMO, methane monooxygenase; MMOH, MMO hydroxylase component; MMOB, MMO component B; MMOR, MMO reductase component; SHE, standard hydrogen electrode; R2, subunit R2 of *Escherichia coli* ribonucleotide reductase; Hr, hemerythrin.

0006-2960/94/0433-713$04.50/0

The latter studies also showed that the redox state of MMOH at the time immediately preceding oxygen activation strongly influenced the product distribution, suggesting a link between the redox state and reactivity.

Past studies of the redox characteristics of MMOH have been carried out using the enzyme isolated from *Methylococcus capsulatus* Bath (Woodland et al., 1986; Liu & Lippard, 1991a,b). These studies were complicated by the fact that MMOH is essentially colorless in the visible spectral region. Consequently, the extent of reduction was monitored solely by spin quantitation of the characteristic EPR spectrum from the mixed-valence state for which all three g values occur below $g = 2$ ($g_{av} = 1.85$). Despite their similar protocols, the two studies gave quite different results. Woodland et al. (1986) reported formal potential values of +350 and −25 mV for the first and second electron transfers, respectively, with (inexplicably) only 27% maximal formation of the mixed-valence state.[2] In contrast, Liu and Lippard (1991a,b) reported formal redox potential values of +48 and −135 mV for these same two redox couples with 85% formation of the mixed-valence state. The latter group also reported that addition of MMOR and MMOB to MMOH blocked electron transfer to the diiron cluster unless propylene, an alternate substrate, was also present. Although the reasons for the contrasting findings reported for studies are unclear, they may be related to the dependence on absolute quantitation of the EPR spectra of only one of the three redox states of MMOH as a means to determine the extent of overall reduction. This methodology assumes, but does not prove, equilibrium of redox states and accuracy of the spin quantitation.

We have developed techniques that result in preparations of MMOH from *M. trichosporium* OB3b that have approximately twice the diiron cluster content and 10–20-fold higher specific activities than the *M. capsulatus* MMOH preparations used for the previous studies (Fox et al., 1989, 1990b). Using enzyme prepared in this way, EPR and Mössbauer techniques have been developed that allow each redox state of MMOH to be detected and directly quantitated (Fox et al., 1988, 1993; Hendrich et al., 1990). Moreover, special equipment for the combined use of electrochemistry and EPR or Mössbauer spectroscopy in the determination of redox potential values of biomolecules has been developed (Paulsen et al., 1992, 1993). In the present study, the reductive titrations of MMOH alone and in complexes with MMOR, MMOB, and propylene are quantitated using EPR and Mössbauer spectroscopies. In conjunction with the electrochemical studies, these techniques allow each of the redox states of MMOH to be monitored so that accurate potential values can be obtained. We show that the two formal redox potential values of MMOH from *M. trichosporium* are significantly different than those reported for MMOH from the *M. capsulatus* enzyme. Moreover, the redox potential values of MMOH are shown to be affected by component complex formation in a quite different manner than that previously described (Liu & Lippard, 1991a,b). Our findings suggest that the affinities of component complexes are correlated with redox-dependent structural changes in MMOH. The findings are consistent with a scheme in which dissociation and reassociation of the MMOB–MMOH complex are synchronized with the catalytic cycle by the reduction and oxidation of MMOH, thereby allowing MMOB to contribute to the regulation of MMO catalysis.

[2] For a linked redox system, the amount of mixed-valance state is thermodynamically controlled by the separation of the redox potentials for the two electron-transfer reactions. For the case cited here, nearly 100% formation of the mixed-valence state would be expected.

EXPERIMENTAL PROCEDURES

Materials

MMOH, MMOB, and MMOR were purified and characterized from *M. trichosporium* OB3b (Fox et al., 1989, 1990b). Concentrations of protein components were determined by quantitative amino acid analysis, and the iron content of MMOH was determined by inductively coupled plasma emission spectroscopy (Fox et al., 1989). MMOH for Mössbauer experiments was prepared from cells grown in media enriched in ^{57}Fe (95 atom %; Atomergic Chemetals Corp., Farmingdale, NY) (Fox et al., 1989, 1993). The specific activities of the MMOH, MMOB, and MMOR preparations used were 800–1200, 12 000, and 20 000 nmol min^{-1} mg^{-1}, respectively. Iron analysis indicated that two diiron clusters were present per mole of MMOH. Specific activity values are reported for the polarographic determination of furan oxidation as described previously (Fox et al., 1990b).

The chemicals used and their sources are as follows: methyl viologen and gallocyanine (British Drug House); indigo disulfonate (indigo carmine) (Manufacturing Chemists); 2-hydroxy-1,4-naphthoquinone and riboflavin (Eastman Kodak Co.); anthraquinone-1,5-disulfonate, 2,5-dihydroxy-*p*-benzoquinone, and ferrocenecarboxylic acid (Aldrich Chemical Co.); phenazine methosulfate, phenazine ethosulfate, duroquinone (tetramethyl-*p*-benzoquinone), and MOPS [3-(*N*-morpholino)propanesulfonic acid] (Sigma Chemical Co.). 8-Chlororiboflavin was the generous gift of J. P. Lambooy, University of Maryland. 4-Thioriboflavin was the generous gift of Sandro Ghisla, University of Konstanz, West Germany. Pyocyanine was photochemically prepared from phenazine methosulfate according to the method of McIlwain (1937). Water was glass-distilled.

Methods

EPR–Spectroelectrochemical Titrations. The EPR–spectroelectrochemical cell and titration method have been previously described (Paulsen et al., 1992, 1993). A slightly modified cell was made for this study because MMOH exhibits almost no visible absorption spectrum. In place of the cuvette employed in the previous apparatus, the redesigned cell used a cylindrical electrode compartment (1-cm diameter) into which auxiliary, reference, and working electrodes were placed. Since this cell was designed for more efficient stirring, equilibrium was achieved more rapidly than in the previous cell. With this cell, EPR samples were collected under anaerobic conditions, each representative of a single point in the redox titration.

All EPR–spectroelectrochemical experiments were performed using 100 mM MOPS buffer at pH 7.0 and 4 °C with MMOH at 210–340 μM in a starting volume of 1.9 mL. The formal potential value determinations of MMOH complexed to MMOB were performed at stoichiometries of 2.1–2.4 component B per 1.0 MMOH diiron cluster.

Methyl viologen was used to mediate electron transfer in the reductive direction in both the dithionite and electrochemical titrations. Ferrocenecarboxylic acid was used to mediate electron transfer in the oxidative direction. Methyl viologen, ferrocenecarboxylic acid, and all redox indicators, except for duroquinone, were made to a concentration of approximately 20% (80–120 μM) of the concentration of diiron clusters present in each experiment. Duroquinone was only soluble to about 5% of the cluster concentration and was added from a separate saturated solution prepared in 100 mM MOPS at pH 7.0. In order to determine whether the redox indicators

bound to MMOH, the EPR signals of the mixed-valence and fully reduced states of MMOH were observed in the presence of each indicator. Two criteria were used to determine if binding occurred: (i) change in the relative signal shape and intensity of the spectral features; (ii) change in the microwave power saturation characteristics of the EPR spectrum of mixed-valence state.

The midpoint potential values for the following redox indicators were determined by visible–spectroelectrochemical titration under the same conditions used in this work (pH 7.0 and 4 °C): phenazine methosulfate (E_m = +141 mV); phenazine ethosulfate (E_m = +108 mV); gallocyanine (E_m = +76 mV); pyocyanine (E_m = +28 mV); indigo disulfonate (E_m = –46 mV); 2,5-dihydroxy-*p*-benzoquinone (E_m = –81 mV); 2-hydroxy-1,4-naphthoquinone (E_m = –83 mV); 8-chlororiboflavin (E_m = –114 mV); riboflavin (E_m = –158 mV). The midpoint potential values for duroquinone (E_m = +5 mV) and anthraquinone-1,5-disulfonate (E_m = –175 mV) were measured at pH 7.0 and 25 °C (Fultz & Durst, 1982). The midpoint potential value for 4-thioriboflavin (E_m = –7 mV) was measured at 4 °C and adjusted to pH 7.0 (Nishino et al., 1987). The formal potential values for methyl viologen ($E^{\circ\prime}$ = –450 mV) and ferrocenecarboxylic acid ($E^{\circ\prime}$ = +590 mV) (Wilkinson et al., 1952) were measured at pH 7.0 and 25 °C. All redox potentials are reported versus SHE.

Sodium dithionite solutions were prepared to a concentration of 70 mM to minimize dilution during reductive titration. Dithionite was used as the reductant for MMOH in this study because electrochemical reduction (and oxidation) was deemed to be too slow, due to the relatively large concentrations of proteins present in the experimental solution. A typical dithionite titration required 12–15 h and yielded five EPR samples poised at different potential values. Typical equilibration times were 1–2 h per titration point, and equilibrium was assumed to be achieved when the potential was stable for 10–15 min. The protein solution remaining after the titration (approximately 0.5 mL) did not appear turbid, indicating that the protein was not denatured during the titration period. In one case, the redox indicator dyes were removed from this protein solution by gel filtration so that the specific activity of the sample could be assessed using the oxygen electrode method (Fox et al., 1990b). It was found that 83% of the initial specific activity was retained. This is equivalent to the specific activity of a sample treated similarly but not reduced. Potential measurements were made using either a BAS-100 electrochemical analyzer or an Orion Research Model 601A digital ionalyzer as previously described (Paulsen et al., 1992).

Determination of the Relative Redox Potential Values of MMOH Complexes with Other MMO Components and Propylene. MMOH (200 μM) with or without other MMO components and/or propylene was incubated anaerobically with 400 μM concentrations of eight redox indicators in 100 mM MOPS, pH 7.0, 4 °C. These indicators served to buffer the redox potential so that addition of a fixed amount of reductant (dithionite) resulted in approximately the same system potential independent of the midpoint potential of the MMOH complex present. The indicators used were phenazine methosulfate, phenazine ethosulfate, gallocyanine, pyocyanine, indigo disulfonate, 2,5-dihydroxy-*p*-benzoquinone, 2-hydroxy-1,4-naphthoquinone, and methyl viologen. The relative concentrations of MMOH and the other MMO components when present are given in the legend of Figure 4. When required, propylene (8 psi) was added to the head space of a septum-sealed sample vessel and allowed to equilibrate to make a saturated solution. After addition of dithionite, samples were incubated for 1.5 h to allow equilibrium to be established and then frozen in liquid nitrogen.

EPR Instrumentation and Data Analysis. Low-temperature X-band EPR measurements were made using a Varian E-109 spectrometer and an Oxford Instruments ESR-910 liquid helium cryostat (Fox et al., 1989). EPR spectral manipulations and integrations were performed using a program written by Dr. David R. Jollie, University of Minnesota. The standard used for spin quantitation was a 1.0 mM $Cu(ClO_4)_2$ solution. Spin quantitations were performed by double integrations of spectra measured at nonsaturating microwave power levels according to previously described procedures (Aasa & Vänngård, 1975; Fee, 1978; Fox et al., 1991).

Mössbauer Instrumentation and Data Analysis. Mössbauer instrumentation was as previously described (Fox et al., 1993). The relative proportions of the diferric and diferrous states present during the poised potential reductive titrations were determined by spectral subtractions using the Mössbauer parameters previously defined for these states (Fox et al., 1993). The Mössbauer spectrum of the mixed-valence state of MMOH free of MMOB was simulated using an effective $S = {}^1/_2$ spin Hamiltonian assuming a strong coupling limit [see eq 5 of Fox et al. (1993)]. The following adjustments to the previously published parameters were used in the simulations: Fe^{3+} site $A_{eff,i}$ (MHz) (x, y, z), $(-70, -77, -74)$; Fe^{2+} site $A_{eff,i}$ (MHz) (x, y, z), $(38, 34, 27)$; Voight line width, 0.4 mm/s. All other parameters used for the Mössbauer simulations were the same as those previously reported. Mössbauer spectral analyses were performed using WMOSS (Web Research Co., Edina, MN).

Samples used for quantitation by Mössbauer spectroscopy were obtained during an EPR–spectroelectrochemical titration of ^{57}Fe-enriched MMOH. The same electrochemical cell described above for EPR samples was used except that a glass container housing a Mössbauer sample cup was attached to the cell in place of an EPR tube. During the titration of the ^{57}Fe-enriched MMOH, an EPR sample was taken at each titration point, in order to allow comparison of the results obtained from each method of quantitation.

The concentration of the ^{57}Fe-enriched MMOH used to obtain Mössbauer spectra of the partially reduced MMOH and MMOH–MMOB complexes were 694 and 434 μM, respectively, and contained 1.8 and 2.0 diiron clusters per mole of MMOH, respectively. The concentration of MMOB used in the latter experiment was 2.40 mM. All other experimental conditions used for the titrations of ^{57}Fe-enriched MMOH were similar to those used in the EPR–spectroelectrochemical titrations, except that due to the increased protein concentrations, the time allowed for equilibration was increased to 3 h to ensure that equilibrium was achieved.

Calculations. EPR–spectroelectrochemical data were plotted as the fraction of mixed-valence state determined by EPR quantitation versus the measured potential value (E), at each point in the titration and fit by nonlinear regression (Duggleby, 1981) according to the equation:

$$\text{fraction in mixed-valence state} = \frac{1}{1 + \exp[(nF/RT)(E - E_1^{\circ\prime})] + \exp[(nF/RT)(E_2^{\circ\prime} - E)]} \quad (1)$$

where $E_1^{\circ\prime}$ and $E_2^{\circ\prime}$ are the formal potential values for the first and second electron transfers calculated from the program, F is the Faraday constant, R is the gas constant, n is equal to 1, and T is equal to 277 K. The maximum fraction of

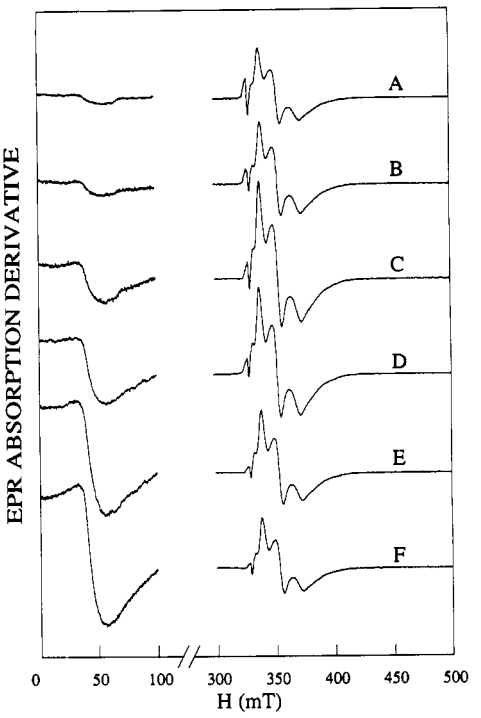

FIGURE 1: X-band EPR spectra recorded during the EPR–spectroelectrochemical titration of MMOH. MMOH (300 μM) in 100 mM MOPS, pH 7.0, 4 °C, was reduced as described under Experimental Procedures. Samples were taken at five different system potential values: (A) +113 mV; (B) +98 mV; (C) +63 mV; (D) +25 mV; (E) +6 mV; (F) −11 mV. X-band EPR spectra were recorded at nonsaturating microwave power. Instrumental conditions for the signal from the mixed-valence state (right portion of the spectra shown) were the following: gain = 6.3×10^3, scan range = 200 mT, scan center = 400 mT, modulation amplitude = 1 mT, modulation frequency = 100 kHz, microwave frequency = 9.21 GHz, microwave power = 10 μW, temperature = 13 K. For the signal from the diferrous state (left portion of the spectra shown), the conditions were as follows: scan range = 100 mT, scan center = 50 mT, gain = 1×10^4, microwave power = 2 mW, temperature = 13 K.

mixed-valence state (M) formed during the titration was calculated from the equation (Clark, 1960):

$$E_1^{\circ\prime} - E_2^{\circ\prime} = 0.110 \log[2M/(1 - M)] \qquad (2)$$

RESULTS

Formal Redox Potential Values of Free MMOH. Low-temperature EPR spectra measured during the potentiometric titration of free MMOH are shown in Figure 1. The resonances below $g = 2$ derive from the mixed-valence state of the enzyme while the resonance near $g = 16$ arises from the (integer spin) diferrous state. The positions, relative intensities, and saturation characteristics of the EPR resonances did not change during the titration, suggesting that the redox indicators used in this study do not perturb the environment of the dinuclear iron cluster. We found this not to be true of two indicators used in previous studies (Woodland et al., 1986; Liu & Lippard, 1991a,b). Both methylene blue and 2,6-dichlorophenolindophenol caused a significant decrease in the half-saturation power of the mixed-valence spectrum. In addition, methylene blue was found to elicit a new resonance in the $g = 2$ region during the titration. Thus, each of these indicators appears to bind to *M. trichosporium* MMOH and change its physical properties.

EPR spectra of the mixed-valence state like those shown in Figure 1 were quantitated by double integration. In Figure 2, the results of these quantitations are plotted versus the

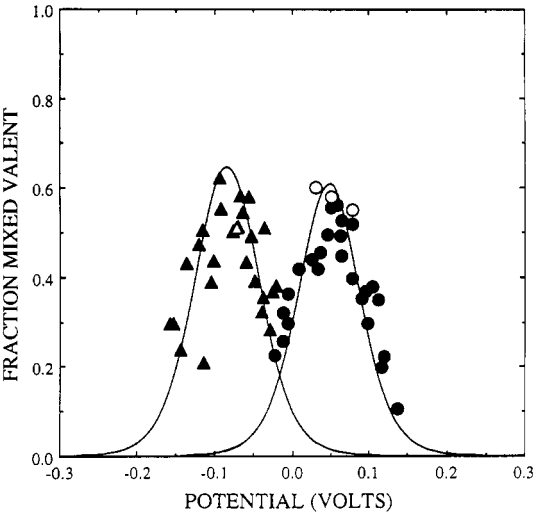

FIGURE 2: Fraction of mixed-valence state stabilized during the reductive titration of MMOH and MMOH–MMOB complex at different system potential values. The fractions of the mixed-valence MMOH state determined by double integration of the EPR signal as described under Experimental Procedures are plotted versus system potential values: MMOH (●); MMOH–MMOB complex (▲). The best fit of the data according to eq 1 are plotted as *solid lines*. The fractions of the mixed-valence MMOH and MMOH–MMOB complex determined by Mössbauer spectroscopy are also shown: MMOH (○); MMOH–MMOB complex (△).

measured system potentials obtained during potentiometric titration. By fitting the data as described under Experimental Procedures, the formal potential values were determined. For MMOH, the values for the first and second electron transfers were $E_1^{\circ\prime} = +76 \pm 15$ mV and $E_2^{\circ\prime} = +21 \pm 15$ mV, respectively, at 4 °C (overall midpoint potential $E_m = +48$ mV). This separation between potential values indicates that the maximum percentage of mixed-valence state that could be thermodynamically stabilized is 61%. The $g = 16$ signal cannot be quantitated in absolute terms without simulation because the resonance has intensity at zero magnetic field, indicating that a significant population of the spins cannot be observed at X-band. However, simulations of this signal in the past have shown that essentially all of the diiron cluster in the diferrous state is accounted for by the state that gives rise to the $g = 16$ signal (Hendrich et al., 1990). Thus, the relative signal intensity can be used to estimate the amount of MMOH in the diferrous state. This determination correlates well with the loss of mixed-valence signal intensity as shown in Figure 1.

Reversibility of MMOH reduction was tested by using ferrocenecarboxylic acid to mediate electron transfer to a gold electrode. The MMOH was partially reduced by dithionite to establish a potential of +66 mV (53.5% mixed-valence) and then reoxidized coulometrically. When potentials of +73 and +76 mV were established, the percentage of mixed-valence state present changed to 40.5% and 35.5%, respectively. A loss of intensity from the EPR resonances of the diferrous state was also observed, indicating that the sample had been reoxidized (data not shown). The sample was then reduced to a system potential of +10 mV. This also resulted in the formation of 35.5% mixed-valence state; however, the sample exhibited substantially more $g = 16$ signal intensity. Thus, the system potential had been set on the opposite side of the E_m potential. Ferricyanide was then used to reoxidize the experimental solution to a potential of +77 mV, resulting in the formation of 26% mixed-valence state and a substantial decrease in $g = 16$ signal intensity. The distribution of redox

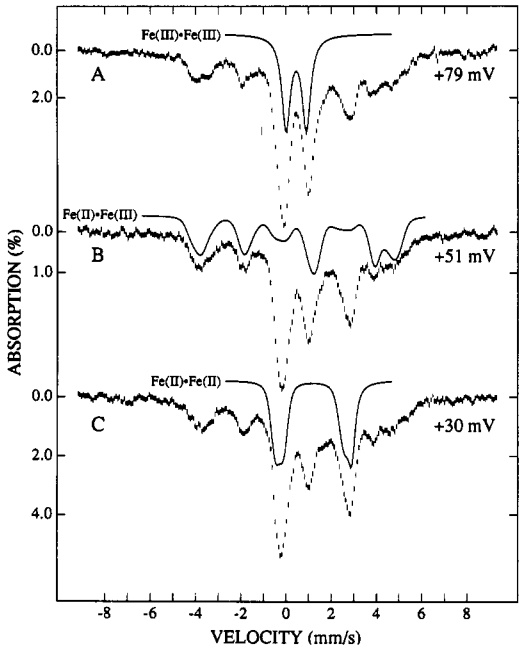

FIGURE 3: Mössbauer spectra of the ^{57}Fe-enriched MMOH poised at the indicated redox potential values recorded at 4.2 K in 45-mT applied field. The reduction of the MMOH cluster and stabilization of system redox potentials were as described under Experimental Procedures. The *solid lines* show the contributions of the indicated redox states of the MMOH diiron cluster based on the previously reported characterizations and simulation procedures (Fox et al., 1993). For each spectrum, the percentages of each redox state were determined by spectral subtractions as described under Experimental Procedures.

states observed for each of these samples correlated well with the function used to fit the MMOH EPR–spectroelectrochemical data shown in Figure 2.[3]

Mössbauer spectroscopy was used to independently determine the distribution of redox states in a sample poised near the E_m value. Figure 3 shows the Mössbauer spectra of samples of the ^{57}Fe-enriched MMOH that were poised between +30 and +79 mV. The data from the poised samples (hatched lines) represent a superposition of the spectra of the three "pure" redox states. During the course of the titration, the relative proportion of each redox state changed. Thus, the spectrum in Figure 3A (+79 mV) is composed primarily of the spectra of the diferric and mixed-valence states, while that of Figure 3C (+30 mV) has a large contribution from the spectra of the mixed-valence and fully reduced states. We have previously characterized the Mössbauer spectra of each redox state of MMOH (Fox et al., 1988, 1993). Quadrupole doublets representing the diferric and diferrous redox states are shown as the solid lines in Figure 3A and Figure 3C, respectively. The percentage of the mixed-valence state present at each redox potential can be determined by subtracting the percentage contributions of the diferric and diferrous states from the total analytically quantitated iron in the samples. Alternatively, the concentration of the mixed-valence state can be determined by direct simulation of the Mössbauer spectrum of the mixed-valence state. The Mössbauer spectrum was simulated (solid line in Figure 3B) using an effective $S = {}^1/_2$ spin Hamiltonian assuming a strong coupling limit [see eq 5 of Fox et al. (1993)]. The percentage

[3] In a separate experiment, electrochemical reduction mediated by methyl viologen was attempted. However, as in the oxidative direction, the system was slow to reduce at the large protein concentrations that were present in the experimental solution.

Table 1: Quantitation of Redox-State Distributions of ^{57}Fe-Enriched MMOH Samples Poised Near the Midpoint Potential[a]

sample no.	E[b] (mV)	EPR[c] mixed valence (%)	Mössbauer[d] diferric (%)	Mössbauer[d] mixed-valence (%)	Mössbauer[d] diferrous (%)
1	79	55	29	55	16
2	51	49	18	58	24
3	30	58	10	60	30

[a] Samples were poised in the spectroelectrochemical titration cell as described under Experimental Procedures. [b] Represents the system redox potential. Values given are relative to SHE. Error ± 5 mV. [c] Determined by double integration of the g_{av} = 1.85 signal as described under Experimental Procedures. Error ± 5%. [d] Determined by fitting the observed spectra with the previously measured spectra of the "pure" states as described under Experimental Procedures and the text. Error ± 5%.

contribution of the mixed-valence state determined from this simulation was found to closely agree with that determined by the spectral subtraction procedures. The percentage of the mixed-valence state determined by Mössbauer spectroscopy is plotted in Figure 2 (open circles) for comparison with the results obtained from the EPR–spectroelectrochemical titration.

The results from the Mössbauer and EPR quantitation of three samples taken during the potentiometric titration of the free ^{57}Fe-enriched MMOH are shown in Table 1. There is good agreement between the values obtained from Mössbauer and EPR quantitation for the fraction of mixed-valence state present in the samples. The results obtained from the Mössbauer quantitation of these samples verify that the maximum amount of mixed-valence state formed during EPR–spectroelectrochemical titration of MMOH is as predicted from the potential separation of the first and second electron formal potential values. The Mössbauer data also indicate that the maximum amount of mixed-valence state was reached during this titration because the ratio of the percentage of diferric to diferrous state in sample 1 is 29:16, but in sample 3 this ratio is 10:30. Thus, the samples were poised at system potentials higher and lower than the E_m value. Moreover, Table 1 shows that the distribution of all three redox states changes in accord with the system potential. This behavior is an excellent indication that the redox species are in thermodynamic equilibrium.

Relative Redox Potential Values of MMOH Complexes with the Other MMO Components and Propylene. A qualitative appraisal of the effects on the E_m value of MMOH complex formation with MMOB, MMOR, and/or the substrate propylene was achieved by adding fixed amounts of dithionite to various component and substrate mixtures. Eight of the redox indicators used in the determination of the formal potential values of MMOH were also added to the solution in stoichiometric amounts relative to the MMOH cluster concentration. At this concentration relative to that of MMOH, these indicators served to buffer the system potential so that it remained nearly constant despite shifts in the state of reduction of MMOH. For the spectra shown in Figure 4, the system potential was equilibrated at approximately −15 mV.[4] As shown in Figure 4A, the MMOH alone under these conditions exhibited both the mixed-valence state (~18% of the cluster concentration) and a substantial amount of the diferrous state (g = 16 EPR signal) as expected from the formal potential values determined in this study. The MMOH in the MMOH–MMOR complex (Figure 4B) exhibited an

[4] At this potential, the cofactors of the MMOR component remained in the oxidized, EPR-silent state.

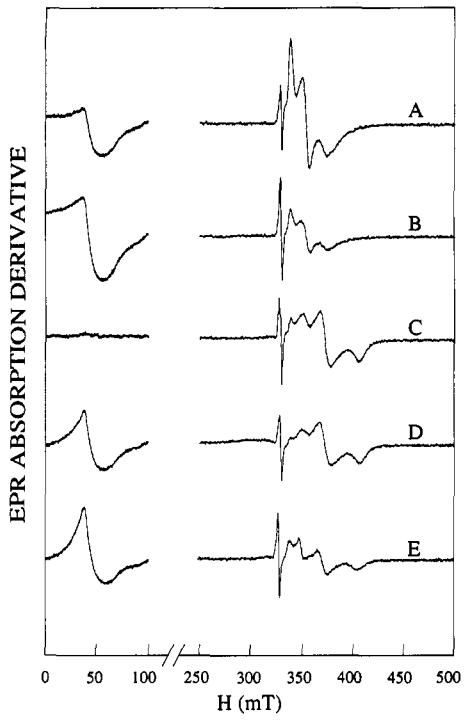

FIGURE 4: X-band EPR spectra of MMOH complexes at a fixed system potential value. Various complexes of MMOH (200 μM) in the presence of a uniform set of indicators were reduced by addition of dithionite as described under Experimental Procedures to establish a system redox potential of approximately −15 mV. The samples were incubated for 1.5 h at 4 °C to allow redox equilibrium to be established. (A) Uncomplexed MMOH; (B) MMOR–MMOH complex at a ratio of 1 MMOR per MMOH diiron cluster; (C) MMOB–MMOH complex at a ratio of 2 MMOB per MMOH diiron cluster; (D) MMOB–MMOR–MMOH complex at a ratio of 2 MMOB and 1 MMOR per MMOH diiron cluster; (E) MMOB–MMOR–MMOH–propylene complex at the same component ratio as (D) and saturated propylene concentration. Instrument conditions for the signal from the mixed-valence state (right portion of the spectra shown) were as follows: gain = 2×10^4, scan range = 250 mT, scan center = 375 mT, modulation amplitude = 1 mT, modulation frequency = 100 kHz, microwave frequency = 9.234 GHz, microwave power = 50 μM, temperature = 8 K. For the signal from the diferrous state (left portion of the spectra shown), the conditions were the following: gain = 2×10^4, scan range = 100 mT, scan center = 50 mT, microwave power = 2 mW, temperature = 8 K.

increase in the $g = 16$ signal and less of the mixed-valence spectrum (~4%) at this system potential, showing that more of the MMOH was in the diferrous state. Thus, it appears that either $E_2°'$ or E_m or both for the complex is more positive than comparable values for MMOH. Interestingly, as shown in Figure 4C, the MMOH in the MMOH–MMOB complex was primarily in the diferric state (~18% mixed-valence state and no apparent $g = 16$ signal from the diferrous state) at this system potential, suggesting a much more negative E_m value than for MMOH alone. In contrast, the MMOH in the MMOH–MMOR–MMOB complex (Figure 4D) exhibited ~7.5% mixed-valence state and a similar concentration of diferrous state as uncomplexed MMOH ($g = 16$ signals are of comparable intensities), suggesting an E_m value similar to MMOH and much more positive than that of the MMOH–MMOB complex. Thus, MMOR binding appears to be the dominant factor in establishing the MMOH redox potential in the ternary component complexes. This was somewhat unexpected because the EPR line shape of the MMOH mixed-valence species in the MMOH–MMOR–MMOB complex is the same as that of the MMOH–MMOB complex (compare Figure 4C and Figure 4D). Thus, the active-site structural changes caused by MMOB binding are retained when MMOR is bound. The addition of the substrate propylene to the ternary complex of the MMO components (Figure 4E) appeared to cause only a small positive shift in the potential, resulting in a slight increase in the extent of reduction and in the intensity of the $g = 16$ signal (compare Figure 4D and Figure 4E). The spectrum from the mixed-valence state in this substrate complex appears as a superposition of the spectrum of the MMOH–MMOR–MMOB complex and that of the mixed-valence MMOH–propylene complex. Thus, the addition of propylene alters the cluster environment, possibly by promoting the dissociation of MMOB.

In the limited study shown here, the MMOR:MMOB:MMOH diiron cluster ratio was established at 1:2:1 with the goal of saturating the MMOH binding sites (Fox et al., 1991). However, a precise determination of the formal redox potential values for MMOH in the ternary component complex will require extensive further study because many different component complexes with different spectral and catalytic properties are known to form at different ratios of components (Fox et al., 1991; Froland et al., 1992). Moreover, a complex is formed between MMOR and MMOB which apparently prevents interaction of these components with MMOH, and this must be taken into account in a detailed analysis. These studies are in progress and will be reported independently.

Formal Redox Potential Values of the MMOH–MMOB Complex. The most dramatic change noted in the survey of the effects of complex formation on MMOH redox potential values summarized in Figure 4 is the large apparent negative shift in E_m caused by the binding of MMOB. Accordingly, the formal potential values of the MMOH–MMOB complex were determined by the same techniques used for MMOH alone. Our past studies have indicated that MMOB profoundly affects many aspects of catalysis through formation of a specific complex with MMOH (Fox et al., 1991; Froland et al., 1992; Lee et al., 1993b). One MMOB per diiron cluster is sufficient to maximize most of the effects. However, large excesses of MMOB are inhibitory (Fox et al., 1991). For the present studies, a sufficient excess of MMOB was added to nearly saturate the MMOH binding site while not forming significant amounts of the inhibitory complexes. As shown in Figure 2, the formal potential values for the first and second electron transfers to MMOH complexed to MMOB (diiron cluster:MMOB ratio = 1:2.25 ± 0.15) were determined to be $E_1°' = -52 \pm 15$ mV and $E_2°' = -115 \pm 15$ mV at 4 °C, respectively. Thus, the average midpoint potential value (−84 mV) becomes 132 mV more negative when MMOH is complexed to component B. Nevertheless, the maximum amount of mixed-valence state obtained during potentiometric titration (65%) is virtually unchanged because the separation of the formal potential values for each electron transfer remains nearly constant.

A potentiometric titration of ^{57}Fe-enriched MMOH complexed to MMOB was also performed for Mössbauer quantitation. A large total protein concentration (3 mM) was necessary in order to provide sufficient diiron cluster for detection by Mössbauer spectroscopy while maintaining a stoichiometry of MMOB to MMOH similar to that used in the EPR–spectroelectrochemical titrations. As a result, it was not possible to precisely measure the system redox potential due to slow equilibration of the system in solution and/or at the electrode surface. Mössbauer spectra of several samples poised near the E_m value of the complex were measured. A progressive shift from diferric to diferrous cluster in this redox potential range was noted, in qualitative agreement with the EPR–spectroelectrochemical titration. The sample poised at

the most negative system potential studied showed a ratio of the percentage of diferric to diferrous redox states of 27:22, indicating that the maximum amount of mixed-valence species had not been achieved. The relative percentage of mixed-valence state in this sample is plotted in Figure 2 (open triangle) at the potential best fit by the distribution of all three redox states (−72 mV). Although less definitive than the analogous Mössbauer data for the titration of MMOH alone, the results show that the midpoint potential is shifted strongly negative relative to uncomplexed MMOH. Moreover, the results indicate that both the distribution of redox states and the maximum amount of mixed-valence state indicated by the EPR–spectroelectrochemical titration results can, in fact, be achieved.

DISCUSSION

Catalysis by the reconstituted MMO system requires redox cycling of the diiron cluster of MMOH. Our past studies have shown that only the diferrous state of the cluster can interact with O_2 to initiate catalysis (Fox et al., 1989; Lee et al., 1993b). The cluster is then transiently oxidized to the [Fe(IV)·Fe(IV)] state (Lee et al., 1993a,b) apparently in conjunction with the formation of an activated oxene intermediate (Fox et al., 1990a). This intermediate is thought to abstract a hydrogen atom from hydrocarbon substrates to yield an intermediate substrate radical and a [Fe(III)·Fe(IV)]–OH cluster (Priestley et al., 1992). Finally, the substrate radical abstracts the cluster-bound hydroxyl group to form the product and leave the cluster once again in the diferric state. The MMOR and MMOB components strongly affect both the rate at which this cycle occurs and the stability of the reaction cycle intermediates (Fox et al., 1989; 1991; Lee et al., 1993b). In this study, we have determined the formal potential values for the reduction reaction that initially brings MMOH into the reactive diferrous state. Moreover, we have shown that these potential values are affected by the formation of complexes between MMOH and the other MMO components. These studies now permit a comparison of the redox behavior of the high-activity MMO system isolated from *M. trichosporium* described here with that of the corresponding enzyme isolated from *M. capsulatus* as well as other proteins containing structurally related diiron clusters. Our findings offer insight into the interaction of MMOH with MMOB and MMOR which may have an important bearing on the function of these components in MMO catalysis. Each of these aspects is discussed in the following sections.

Comparison with Studies of MMOH from M. capsulatus. The two previous studies of the formal redox potential values of MMOH from *M. capsulatus* Bath (Woodland et al., 1986; Liu & Lippard 1991a,b) yielded quite different values for both E_m and the formal potential values of the individual electron-transfer steps. These studies were conducted with enzyme of similar specific activity purified from bacteria from the same original isolate. Thus, it is unlikely that the enzymes were significantly different. Moreover, both studies used the same set of 12 redox indicators, the same source of reducing equivalents, and the same method to quantitate the mixed-valence state. The study of Liu and Lippard (1991a,b) showed a much more reasonable correlation between the measured formal potential values ($E_1°' = +48$ and $E_2°' = -135$ mV, pH 7.0, 25 °C) and the maximum percent observed in the mixed-valence state (85%). Thus, it is likely that the redox potentials reported in the study are more representative of the values at thermodynamic equilibrium. However, this set of redox potential values, in particular the value for $E_2°'$, differs from the values determined in the present study by a much larger amount than can be accounted for by the difference in the temperature at which the determinations were made (ΔT = 21 °C).[5] This may reflect differences in the proteins themselves, since the bacteria from which they were isolated differ in many other morphological and metabolic respects. However, the MMOH components from *M. trichosporium* and *M. capsulatus* appear essentially identical spectroscopically and have very similar amino acid sequences (Stainthorpe et al., 1990; Cardy et al., 1991) and substrate specificities (Green et al., 1989; Froland et al., 1992; Fox et al., 1990a). Indeed, the major difference between the two enzymes appears to be the much higher specific activity and diiron cluster content of MMO from *M. trichosporium.*

One possible source of error in any redox study conducted using redox indicators is the potential for interaction of the indicators with the protein, thereby changing the redox properties of the protein through complex formation. For an enzyme with a broad substrate range like MMO, this may be a significant problem. The indicators employed in the current study showed no effects on the EPR spectral properties of the mixed-valence state. This redox state has been shown to be sensitive to interactions between exogenous molecules and the cluster (Hendrich et al., 1992; Fox et al., 1990c), suggesting that no member of the current set of indicators binds in a manner that perturbs the diiron cluster. In contrast, we observed that two of the indicators used in both previous determinations of the redox potential values of the *M. capsulatus* enzyme caused significant alteration in the EPR spectra of the *M. trichosporium* enzyme. If this is also true for the *M. capsulatus* enzyme, then some error in the earlier measurements may have been introduced. Accordingly, close inspection of the EPR spectra reported for *M. capsulatus* [see Figure 1 of Liu and Lippard (1991a)] reveals a line-shape change as the system potential is decreased.

Another possible source of error in the past studies has been the dependence on quantitation of a single EPR active state as a means to monitor reduction. EPR quantitations are rarely more accurate than ±5%. Moreover, in the case of MMOH, these quantitations must be related to an independent quantitation of the total iron, because the mixed-valence species is never formed in 100% yield. Unfortunately, total iron is not necessarily indicative of the total diiron cluster concentration due to the potential presence of adventitious iron. In the current study, we have addressed these problems through the use of Mössbauer spectroscopy which can uniquely (i) resolve the spin-coupled cluster iron from adventitious iron and (ii) readily yield a quantitation of all three redox states of the MMOH diiron cluster in a single sample.

A third possible source of error in redox measurements of this system stems from the relatively long time required for the MMOH to reach thermodynamic equilibrium with the redox indicators. In past studies, a constant time of 10 min was used (Liu & Lippard, 1991a,b). For the *M. trichosporium* MMOH, we found that the measured system redox potential continued to change for times substantially longer than 10 min after addition of dithionite to establish most potential values. Consequently, in the current study, we used an equilibration time of at least 1 h which proved to be adequate

[5] The change in system potential caused by an increase in the equilibrium temperature from 4 to 25 °C for the indicator mixture used was found to be 6 mV. No significant change in the intensities of the EPR spectra of diferrous and mixed-valence MMOH was observed for identical samples incubated at these two temperatures and then rapidly frozen.

over the entire redox potential range. The redox behavior of the system poised in this way was shown to be reversible in both the oxidative and reductive directions. Moreover, Mössbauer spectroscopy of several samples poised at different potential values showed the expected distributions of redox states based on the determined formal redox potential values indicating that equilibrium had been established.

It is shown here that the formation of a complex with MMOB caused the E_m value of MMOH to shift 132 mV more negative. However, addition of MMOR with or without MMOB and propylene apparently caused only small changes in the redox potential values, resulting in more diferrous and less mixed-valence MMOH at a given system potential. These results are in direct contrast to the results reported for the *M. capsulatus* MMO components (Liu & Lippard, 1991a,b). In the latter case, the addition of MMOR and MMOB as an unresolved mixture to MMOH resulted in a complex that could not be reduced at system potential values as negative as −200 mV, indicating either a kinetic block to reduction or a very negative E_m value. Addition of propylene to this complex allowed the MMOH to be reduced. In fact, only the EPR spectrum of the diferrous state was observed during the redox titration, suggesting that $E_2°'$ was much more positive than $E_1°'$ in this complex. It was proposed for the *M. capsulatus* MMO system that substrate binding may regulate the redox potential of the MMOH in the system so that electron transport can only occur when substrate is present. In contrast, in the *M. trichosporium* system, the MMOH is readily reducible in all of the complexes studied here, but especially so when MMOR is present. The complex of all three components apparently does not have a substantially more negative potential than MMOH alone as reported for *M. capsulatus*. Since the addition of propylene causes only a relatively small change in the extent of reduction of the ternary complex at a fixed system potential, substrate binding is unlikely to be a major mechanism of thermodynamic regulation for the MMO system. Moreover, the mixed-valence state is evident in the EPR spectrum of partially reduced samples of all the component complexes studied here with or without propylene present. This suggests that, if $E_2°'$ is more positive than $E_1°'$ in any of these complexes, the separation between the formal redox potential values is not great.

Comparison with Other Proteins and Enzymes Containing Diiron Clusters. X-ray crystal structures and measurements of the formal redox potential values have been reported for hemerythrin (Stenkamp et al., 1984; Armstrong et al., 1983), ribonucleotide reductase R2 subunit (Nordlund et al., 1990; Lam et al., 1990), and several inorganic model complexes [reviewed in Que and True (1990)]. Although both Hr and R2 contain diiron clusters, the redox potential of hemerythrin ($E_m \sim +210$ mV) is considerably more positive than that reported for R2 ($E_m \sim -110$ mV). The model studies indicate that the redox potential of the diiron cluster becomes more negative as the number of oxyanion versus nitrogen ligands increases. Accordingly, the nonbridging ligands of the iron coordination of diferric Hr are all histidine while those of diferric R2 are a mixture of histidine, carboxylate, and solvent. Another important determinant of the redox potential of the cluster is the nature of the substituents bound to the oxygen atom bridging the two iron atoms. The model studies indicate that protonation or other substitution of the oxygen (*e.g.*, oxyanions such as phenoxy or carboxylate bridging ligands) also causes a positive shift in the redox potential values (Que & True, 1990; Wang et al., 1991). The oxygen bridges of both Hr and R2 in the diferric state are not substituted (Stenkamp et al., 1984; Nordlund et al., 1990; Scarrow et al., 1987; Wilkins & Wilkins, 1987). However, the oxo bridge of Hr becomes substituted in the mixed-valence and diferrous states (Muhoberac et al., 1980; Reem & Solomon, 1987). Unfortunately, nothing is known about the nature of the bridge in the more reduced states of R2. Consequently, the effects of the state of substitution of the bridging oxygen cannot yet be evaluated in the case of these proteins. Other factors such as the accessibility of the cluster to solvent and the presence of dipolar effects due to the secondary structure present in the cluster environment may also strongly affect the observed redox potential. These are particularly important factors in the case of proteins and may dominate the other factors influencing the redox potential values.

The structure of the diiron cluster of MMOH appears to be more closely related to that of R2 than hemerythrin. A limited region of sequence homology with the crystallographically determined cluster binding region of R2 has been noted for the α subunit of MMOH (Nordlund et al., 1992). This alignment predicts that each iron of the MMOH cluster will have a single histidine ligand and several carboxylate oxyanion ligands. The presence of at least one N ligand for each iron has been directly demonstrated using ENDOR spectroscopy (Hendrich et al., 1992; Thomann et al., 1993). In the absence of other environmental effects, this structure for MMO would suggest a relatively negative redox potential value like that of R2. However, MMOH differs from R2 in that the bridging moiety in both the oxidized and mixed-valence states is substituted, probably by hydrogen (DeRose et al., 1993; Thomann et al., 1993; Ericson et al., 1988; DeWitt et al., 1991; Fox et al., 1988, 1993). Such substitution would be expected to increase the redox potential. Thus, the midpoint potential value of MMOH ($E_m = +48$ mV) might be expected to be between those of hemerythrin and R2, which is the case. It is possible that the further negative shift in the midpoint redox potential value caused by MMOB binding to MMOH is due to a change in the iron ligation or the state of substitution of the oxygen bridge.[6] However, other effects such as a change in the solvent accessibility or the structure of the cluster environment caused by a conformational change occurring due to MMOB binding could also account for the decrease in redox potential. Indeed, past spectroscopic studies have demonstrated that the cluster environment is altered when the MMOB–MMOH complex forms as discussed below (Fox et al., 1991; Froland et al., 1992).

It is interesting to note that even though the endogenous ligand structures of the clusters in the R2 subunit and MMOH appear to be similar, the enzymes differ significantly in the amount of mixed-valence state stabilized during reductive titration. Very little mixed-valence state can be stabilized for R2 by direct titration. This indicates that the redox potential values for the first and second electron transfers are reversed in relative magnitude for the two proteins. We do not at present understand the structural basis for this observation.

[6] Although substitution of the oxygen bridge in the MMOB–MMOH complex has not been directly investigated, some results suggest that the degree of substitution does not decrease relative to that of MMOH alone. First, the magnitude of the hyperfine coupling constant J for the antiferromagnetic coupling of the mixed-valence state of MMOH decreases 6-fold when the MMOB–MMOH complex forms (Fox et al., 1991). This decrease in the J value is not consistent with a decrease in substitution of the bridging oxygen. Second, the diferrous clusters of both MMOH and the MMOB–MMOH complex exhibit ferromagnetic coupling indicating that the bridge is substituted (perhaps disubstituted) in each case.

Mechanistic Significance of the Effects of MMOR and MMOB on the MMOH Redox Potential Values. In past studies, we have demonstrated the importance of component complexes in catalysis by the MMO system (Fox et al., 1991; Froland et al., 1992). The fact that the effects of these complexes did not all exhibit the same dependence on component concentration showed that the components have more than one role in catalysis. For example, the rate of steady-state turnover by the reconstituted system appears to depend upon the extent of formation of a complex containing stoichiometric amounts of MMOR and MMOB per MMOH diiron cluster (Fox et al., 1991). In contrast, as little as 0.1 MMOB per MMOH active site maximally shifts the distribution of products observed for several substrates that can be oxidized in more than one poisition in MMOH-catalyzed reactions (Froland et al., 1992). There are also several indications that the structure or environment of the MMOH diiron cluster is altered in the MMOB complex and that the dissociation constant is affected by the redox state of the cluster. For example, the EPR spectrum of the mixed-valence state of MMOH is progressively altered until a stoichiometric complex with MMOB forms, consistent with a high-affinity complex. In contrast, analogous changes in the EPR spectrum of diferrous MMOH maximize at 0.3 MMOB per cluster. This is thought to result from hysteresis in the relaxation of the altered structure of MMOH in solution after a weakly bound MMOB dissociates. Thus, a relatively small amount of MMOB can affect the entire diferrous MMOH population so long as the dissociation rate of MMOB is fast and the hysteresis time is long compared to the freezing time for the EPR sample (Froland et al., 1992). On the basis of these and related observations, we have proposed a regulatory scheme in which MMOB first functions to facilitate electron transport from MMOR to MMOH in a stoichiometric complex and then, at a later point in the catalytic cycle, plays a second role related to assuring tight coupling between O_2 activation and substrate oxidation (Froland et al., 1992; Fox et al., 1991). For example, this second function of MMOB might be fulfilled by cyclic dissociation and reassociation at appropriate points in the catalytic cycle so that (i) access of the substrate to the MMOH diiron cluster is restricted until the cluster is reduced or oxygen is activated and (ii) product release is promoted by MMOB reassociation. The current results present a mechanism by which the affinity of the MMOB–MMOH complex might be coupled to the catalytic cycle of MMOH. As shown in Figure 5, the 132-mV decrease in the E_m of MMOH associated with MMOB binding indicates approximately a 4–5 order of magnitude decrease in the affinity between these components upon reduction of the MMOH. Steady-state kinetic studies (Fox et al., 1991) and preliminary binding studies[7] suggest that the MMOB–MMOH complex has a binding constant of ~8 nM (23 °C). However, upon reduction of MMOH, the dissociation constant increases by at least 3–4 orders of magnitude,[7] in accord with the thermodynamic relationships shown in Figure 5. Thus, at the onset of the catalytic cycle, and at the concentrations of components typically found *in vivo*, a strong stoichiometric complex between MMOH and MMOB would form as required for efficient steady-state turnover. However, after reduction occurs, a decrease in MMOB affinity would permit dissociation of the component complexes for regulatory purposes of the type described above.

In contrast to the effects of MMOB, MMOR appears to cause only small changes in the redox potential of MMOH upon complex formation. However, it does appear to be able to interfere with the coupling between the MMOB binding energy and the redox potential of MMOH. Thus, MMOB may retain high affinity for diferrous MMOH as long as MMOR is bound, and dissociation of MMOR may be the event that initiates the dissociation of the MMOB–MMOH complex. If this sequence of events is correct, then the decrease in redox potential associated with the MMOB–MMOH complex would occur after reduction of the diiron cluster, and therefore have no effect on the reduction process. Thus, the decrease in redox potential may simply be a reflection of the decreased affinity between components. However, the decreased redox potential may also have mechanistic significance in that the more negative potential of the MMOB–MMOH complex would facilitate O_2 reduction and activation by the diiron cluster.

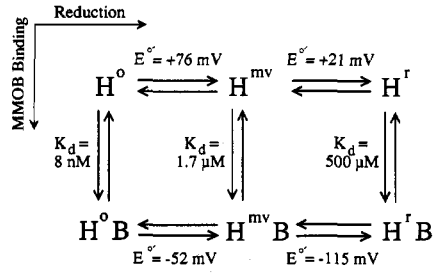

FIGURE 5: Thermodynamic energy coupling of the MMOH reduction and MMOB binding process. MMOH (H^o) can be reduced to the mixed-valence (H^{mv}) and diferrous (H^r) states. Each of these states can bind MMOB, but the MMOB-dependent shift in redox potential values requires that the affinity of the MMOH–MMOB complex be dependent upon the redox state of MMOH. The calculations are based on the formal redox potential values measured here and a measurement of the K_d value for the diferric MMOH–MMOB complex.[7] The latter value was measured at 23 °C; thus, some shift in the absolute but not the relative magnitude of the potential values and dissociation constants is expected for values measured at a single temperature.

The relative molar amount of MMOR in the cell appears to be only about 10% of the amounts of MMOB and MMOH based on assays of cell-free extracts and the recovery of the individual components observed from purification procedures (Fox et al., 1989). Accordingly, the homogeneous MMOR has about 10 times the specific activity of MMOH. Thus, it seems likely that a single MMOR provides electrons for several MMOH molecules and probably dissociates and reassociates relatively rapidly. This would allow both efficient distribution of reducing equivalents to the entire population and efficient cycling of MMOH, if MMOR and MMOB dissociations are linked as we proposed. However, dynamic measurements of the dissociation rates of MMO component complexes are required before the role of these complexes can be described in more detail.

Relationship to Thermodynamic Regulation in Other Monooxygenase Systems. In studies of the regulation of cytochrome $P450_{cam}$ (Sligar & Gunsalus, 1974), as well as studies of MMO from *M. capsulatus* (Liu & Lippard, 1991a,b), the coupling of binding and redox energies of components and substrates have been proposed to provide a redox switch that inhibits electron transport in the absence of a substrate. In the case of MMO from *M. trichosporium*, this does not seem to be the case because the redox potentials of MMOH in all complexes studied are well above the redox potentials of both redox-active groups of MMOR (Lund & Dalton, 1985; Prince & Patel, 1986). Thus, if the coupling of redox and binding energy in the *M. trichosporium* system is to have a role in catalysis, it is more likely to be in coordination

[7] Y. Liu and J. D. Lipscomb, unpublished results.

of the involvement of component interactions in the chemistry of the catalytic cycle as we have proposed here.

REFERENCES

Aasa, R., & Vänngård, T. (1975) *J. Magn. Reson. 19*, 308–315.

Andersson, K. K., Froland, W. A., Lee, S.-K., & Lipscomb, J. D. (1991) *New J. Chem. 15*, 411–415.

Armstrong, F. A., Harrington, P. C., & Wilkins, R. G. (1983) *J. Inorg. Biochem. 18*, 83–91.

Cardy, D. L. N., Laidler, V., Salmond, G. P. C.; & Murrell, J. C. (1991) *Mol. Microbiol. 5*, 335–342.

Clark, W. M. (1960) *Oxidation–Reduction Potentials of Organic Compounds*, pp 185–187, Robert E. Krieger Co., Huntington, NY.

DeRose, V. J., Liu, K. E., Kurtz, D. M., Hoffman, B. M., & Lippard, S. J. (1993) *J. Am. Chem. Soc. 115*, 6440–6441.

DeWitt, J. G., Bentsen, J. G., Rosenzweig, A. C., Hedman, B., Green, J., Pilkington, S., Papaefthymiou, G. C., Dalton, H., Hodgson, K. O., & Lippard, S. J. (1991) *J. Am. Chem. Soc. 113*, 9219–9235.

Duggleby, R. G. (1981) *Anal. Biochem. 110*, 9–18.

Ericson, A., Hedman, B., Hodgson, K. O., Green, J., Dalton, H., Bentsen, J. G., Beer, R. H., & Lippard, S. J. (1988) *J. Am. Chem. Soc. 110*, 2330–2332.

Fee, J. A. (1978) *Methods Enzymol. 49*, 512–528.

Fox, B. G., & Lipscomb, J. D. (1990) in *Biological Oxidation Systems* (Reddy, C., Hamilton, G., & Madyastha, M., Eds.) Vol. I, pp 367–388, Academic Press, Orlando, FL.

Fox, B. G., Surerus, K. K., Münck, E., & Lipscomb, J. D. (1988) *J. Biol. Chem. 263*, 10553–10556.

Fox, B. G., Froland, W. A., Dege, J. E., & Lipscomb, J. D. (1989) *J. Biol. Chem. 264*, 10023–10033.

Fox, B. G., Borneman, J. G., Wackett, L. P., & Lipscomb, J. D. (1990a) *Biochemistry 29*, 6419–6427.

Fox, B. G., Froland, W. A.; Jollie, D., & Lipscomb, J. D. (1990b) *Methods Enzymol. 188*, 191–202.

Fox, B. G., Froland, W. A., & Lipscomb, J. D. (1990c) in *Gas, Oil and Coal Biotechnology* (Akin, C., & Smith, J., Eds.) Vol. 1, pp 197–214, Institute of Gas Technology Press, Chicago, IL.

Fox, B. G., Liu, Y., Dege, J. E., & Lipscomb, J. D. (1991) *J. Biol. Chem. 266*, 540–550.

Fox, B. G., Hendrich, M. P., Surerus, K. K., Andersson, K. K., Froland, W. A., Lipscomb, J. D., & Münck, E. (1993) *J. Am. Chem. Soc., 115*, 3688–3701.

Froland, W. A., Andersson, K. K., Lee, S.-K., Liu, Y., & Lipscomb, J. D. (1992) *J. Biol. Chem. 267*, 17588–17597.

Fultz, M. L., & Durst, R. A. (1982) *Anal. Chim. Acta 140*, 1–18.

Green, J., & Dalton, H. (1989) *J. Biol. Chem. 264*, 17698–17703.

Hendrich, M. P., Münck, E., Fox, B. G., & Lipscomb, J. D. (1990) *J. Am. Chem. Soc. 112*, 5861–5865.

Hendrich, M. P., Fox, B. G., Andersson, K. K., Debrunner, P. G., & Lipscomb, J. D. (1992) *J. Biol. Chem. 267*, 261–269.

Higgins, I. J., Best, D. J., & Hammond, R. C. (1980) *Nature 286*, 561–564.

Lam, K.-Y., Fortier, D. G., & Sykes, A. G. (1990) *J. Chem. Soc., Chem. Commun.*, 1019–1021.

Lee, S.-K., Fox, B. G., Froland, W. A., Lipscomb, J. D., & Münck, E. (1993a) *J. Am. Chem. Soc. 115*, 6450–6451.

Lee, S.-K., Nesheim, J. C., & Lipscomb, J. D. (1993b) *J. Biol. Chem. 268*, 21569–21577.

Liu, K. E., & Lippard, S. J. (1991a) *J. Biol. Chem. 266*, 12836–12839.

Liu, K. E., & Lippard, S. J. (1991b) *J. Biol. Chem. 266*, 24859.

Lund, J., & Dalton, H. (1985) *Eur. J. Biochem. 147*, 291–296.

McIlwain, H. (1937) *J. Chem. Soc. 2*, 1704–1711.

Muhoberac, B. B., Wharton, D. C., Babcock, L. M., Harrington, P. C., & Wilkins, R. G. (1980) *Biochim. Biophys. Acta 626*, 337–345.

Nishino, T., Nishino, T., & Tsushima, K. (1987) in *Flavins and Flavoproteins* (Edmondson, D. E., & McCormick, D. B., Eds.) pp 417–420, de Gruyter, Berlin.

Nordlund, P., Sjöberg, B.-M., & Eklund, H. (1990) *Nature 345*, 593–598.

Nordlund, P., Dalton, H., & Eklund, H. (1992) *FEBS Lett. 307*, 257–262.

Paulsen, K. E., Orville, A. M., Frerman, F. E., Lipscomb, J. D., & Stankovich, M. T. (1992) *Biochemistry 31*, 11755–11761.

Paulsen, K. E., Stankovich, M. T., & Orville, A. M. (1993) *Methods Enzymol. 227*, 396–411.

Priestley, N. D., Floss, H. G., Froland, W. A., Lipscomb, J. D., Williams, P. G., & Morimoto, H. (1992) *J. Am. Chem. Soc. 114*, 7561–7562.

Prince, R. C., & Patel, R. N. (1986) *FEBS Lett. 203*, 127–130.

Que, L., Jr., & True, A. E. (1990) *Prog. Inorg. Chem. 38*, 97–201.

Reem, R. C., & Solomon, E. I. (1987) *J. Am. Chem. Soc. 109*, 1216–1226.

Scarrow, R. C., Maroney, M. J., Palmer, S. M.; Que, L., Jr., Roe, A. L., Salowe, S. P., & Stubbe, J. (1987) *J. Am. Chem. Soc. 109*, 7857–7864.

Sligar, S. G., & Gunsalus, I. C. (1974) *Proc. Natl. Acad. Sci. U.S.A. 71*, 3906–3910.

Stainthorpe, A. C., Lees, V., Salmond, G. P. C., Dalton, H., & Murrell, J. C. (1990) *Gene 91*, 27–34.

Stenkemp, R. E., Sieker, L. C., & Jensen, L. H. (1984) *J. Am. Chem. Soc. 106*, 618–622.

Thomann, H., Bernardo, M., McCormick, J. M., Pulver, S., Andersson, K. K., Lipscomb, J. D., & Solomon, E. I. (1993) *J. Am. Chem. Soc. 115*, 8881–8882.

Wang, D. L., Holz, R. C., David, S. S., Que, L., Jr., & Stankovich, M. T. (1991) *Biochemistry 30*, 8187–8194.

Wilkins, P. C., & Wilkins, R. G. (1987) *Coord. Chem. Rev. 79*, 195–214.

Wilkinson, G., Rosenblum, M., Whiting, M. C., & Woodward, R. B. (1952) *J. Am. Chem. Soc. 74*, 2125–2126.

Woodland, M. P., Patil, D. S., Cammack, R., & Dalton, H. (1986) *Biochim. Biophys. Acta 873*, 237–242.